

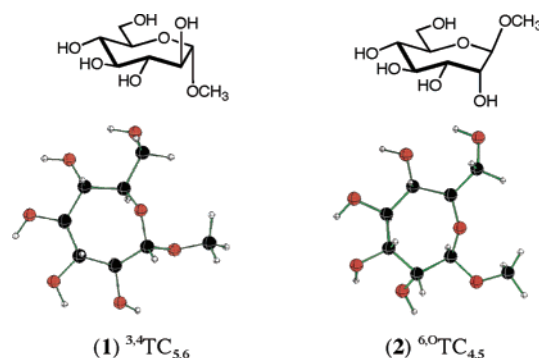
Septanose Carbohydrates: Synthesis and Conformational Studies of Methyl α -D-glycero-D-Idoseptanoside and Methyl β -D-glycero-D-Guloseptanoside

Matthew P. DeMatteo,[†] Nicole L. Snyder,[‡] Martha Morton,[‡] Donna M. Baldisseri,[§] Christopher M. Hadad,^{*,†} and Mark W. Pecuh^{*,‡}

Department of Chemistry, The Ohio State University, 100 West 18th Avenue, Columbus, Ohio 43210,
Department of Chemistry, The University of Connecticut, 55 North Eagleville Road,
Storrs, Connecticut 06269, and BrükerBioSpin Corporation, 15 Fortune Drive, Manning Park,
Billerica, Massachusetts 01821

mark.pecuh@uconn.edu

Received June 24, 2004



We report the synthesis of methyl α -D-glycero-D-idoseptanoside (**1**) and methyl β -D-glycero-D-guloseptanoside (**2**) and the characterization of their preferred solution conformations by computational chemistry and ^1H NMR $^3J_{\text{H,H}}$ coupling constant analysis. Central to the synthetic approach was the epoxidation of glucose-derived oxepine **3** using DMDO. Nucleophilic attack on the resulting 1,2-anhydroseptanose using NaOCH_3 in CH_3OH followed by deprotection provided the 1,2-trans diastereomers **1** and **2**. The computational approach for determining the preferred low energy septanose conformations began with a pseudo Monte Carlo search for each isomer using minimization with the AMBER force field. Single-point energy calculations (HF/6-31G* and B3LYP/6-31+G**) as well as full geometry optimizations in a model for aqueous solvent were then conducted using the conformers within 5 kcal/mol of the AMBER global minimum. Calculated $^3J_{\text{H,H}}$ values, based on a Boltzmann distribution of the computed low energy conformers, were compared to experimental $^3J_{\text{H,H}}$ values from ^1H NMR coupling constant analyses. The correlation between calculated and observed values suggest that septanose carbohydrates are not so flexible and should generally prefer one twist-chair (TC) conformation.

I. Introduction

There is growing interest in the development of size-expanded analogues of natural biopolymers that can interact predictably with biological systems.¹ The new, unnatural oligomers that are the result of these investigations are instrumental for the exploration of cellular

processes and the manipulation of biological pathways using designed molecules. Expanded nucleic acid² and protein³ analogues have been reported, and both have yielded interesting new oligomeric structures with novel biological activity. The common theme in these strategies

(2) (a) Eschenmoser, A. *Science* **1999**, *284*, 2118. (b) Liu, H.; Gao, J.; Lynch, S. R.; Saito, D.; Maynard, L.; Kool, E. T. *Science* **2003**, *302*, 868.

(3) (a) Porter, E. A.; Weisblum, B.; Gellman, S. H. *J. Am. Chem. Soc.* **2002**, *124*, 7324. (b) Porter, E. A.; Wang, X.; Lee, H.-S.; Weisblum, B.; Gellman, S. H. *Nature* **2000**, *404*, 585. (c) Gellman, S. H. *Acc. Chem. Res.* **1998**, *31*, 173. (b) Gademan, K.; Ernst, M.; Hoyer, D.; Seebach, D. *Angew. Chem., Int. Ed.* **1999**, *38*, 1223.

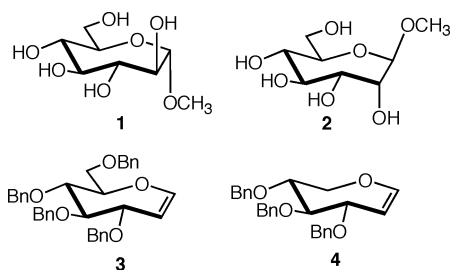
[†] The Ohio State University.

[‡] The University of Connecticut.

[§] BrükerBioSpin Corp.

(1) (a) Rawls, R. L. *Chem. Eng. News* **2000**, *78*, 49. (b) Benner, S. A. *Nature* **2003**, *421*, 118.

CHART 1



has been the homologation of natural monomer residues by one carbon and their subsequent oligomerization. The homologation of natural carbohydrates to create similar size-expanded analogues has received less attention. Septanose carbohydrates, such as **1** and **2**, are homologues of pyranoses in which the sugar ring is expanded by one atom (Chart 1). Just as in the nucleic acid and protein systems, septanose carbohydrates should provide interesting new molecular structures and biological activity. The major obstacles to the utilization of ring-expanded (septanose) carbohydrates for chemical or biological applications are the current inability to easily prepare these molecules as well as our insufficient understanding of their low energy conformations in solution. Implicit to the synthetic challenge is to develop septanose monosaccharides that can participate as donors in glycosylation reactions. The synthesis and conformational analysis of methyl α -D-glycero-D-idoseptanoside (**1**) and methyl β -D-glycero-D-guloseptanoside (**2**) reported here is our starting point to address these challenges.

Previous investigations on septanoses have focused largely on the preparation of monoseptanosides.⁴ Cyclization of pyranoses through the C₆ hydroxyl group to form a seven-membered ring was central to many of the strategies. Selective epimerization of protected glucoseptanosides⁵ prepared from the C₆ cyclization route have provided L-ido,⁶ L-altro, D-gulo, and D-galactoseptanosides.⁷ A variation of the cyclization approach has been used to prepare pyranosyl septanosides.⁸ Acyclic chlorothioethyl acetals were used as donors in glycosylation reactions to give mixed *O,S*-acetals. The primary alcohol at C₆ of the erstwhile donor was then selectively deprotected and used in the cyclization to give pyranosyl septanoside products. The structural consequence of these examples is that the septanose products lack an exocyclic hydroxymethyl group. The exocyclic hydroxymethyl group is characteristic of many natural pyranose and furanose monosaccharides, and we suspect that it may be important for the mimicry of natural pyranoses. Our strategy for the homologation of pyranose sugars relies on oxepines, such as **3**, and leaves the C₆ functionality intact.⁹ We consider carbohydrate-based oxepines

to be ring-expanded glycols that allow for the synthesis of a variety of septanose donors and glycoconjugates. In fact, toward this end, we have recently reported the oxidative coupling of oxepine **4** with a number of nucleophiles.¹⁰

At the outset, we endeavored to prepare monoseptanosides that contained an exocyclic hydroxymethyl group at C₆, such as **1** and **2**, and to determine their preferred low energy conformations. We were interested in elucidating the dominant factors that govern septanose ring conformational analysis, including the anomeric effect, exo-anomeric effect, and a correlation with the different hydroxymethyl rotamers around the C₆–C₇ bond. Particular among these interests was the orientation of the hydroxymethyl group, an issue that has not been addressed prior to this report. The information gathered here provides insight into the conformation of the septanose ring in general and will be used as a starting point for the development of bioactive septanosides.

II. Results

A. Synthetic Methods. The broad utility of glycols in carbohydrate chemistry has motivated our synthetic strategy. Glycols can serve directly as donors under appropriate conditions to form a variety of glycosides;¹¹ they can also be used in the preparation of other classes of donors.¹² We have introduced a synthesis of carbohydrate-based oxepines using a ring-closing metathesis (RCM) strategy.⁹ The route followed other successful precedents of RCM with carbohydrate substrates.¹³ The resulting oxepines (such as **3**, **4**) are seven-membered ring cyclic enol ethers that can serve as glycosyl donors in a similar manner as glycols. Our recent report of the epoxidation of a related D-xylose-based oxepine (**4**) using dimethyldioxirane (DMDO) selectively gave 1,2-anhydro- β -D-idoseptanose and was trapped by a number of nucleophiles to give the corresponding α -idoseptanosides.¹⁰ A key point is that the characterization of the epoxidation stereochemistry in the D-xylose based oxepine (**4**) series was facilitated by comparison of a methyl septanoside derivative to a compound previously reported in the literature.^{6c}

The absence of reference compounds for reactions using the D-glucose-based oxepine (**3**) meant that a similar

(9) Pecuh, M. W.; Synder, N. L. *Tetrahedron Lett.* **2003**, *44*, 4057.

(10) Pecuh, M. W.; Snyder, N. L.; Fyvie, W. S. *Carbohydr. Res.* **2004**, *339*, 1163.

(11) (a) Halcomb, R. L.; Danishefsky, S. J. *J. Am. Chem. Soc.* **1989**, *111*, 6661. (b) Honda, E.; Gin, D. Y. *J. Am. Chem. Soc.* **2002**, *124*, 7343. (c) Kim, J. Y.; Di Bussolo, V.; Gin, D. Y. *Org. Lett.* **2001**, *3*, 303. (d) Friesen, R. W.; Danishefsky, S. J. *J. Am. Chem. Soc.* **1989**, *111*, 6656. (e) Griffith, D. A.; Danishefsky, S. J. *J. Am. Chem. Soc.* **1990**, *112*, 5811. (f) Di Bussolo, V.; Liu, J.; Huffman, L. G., Jr.; Gin, D. Y. *Angew. Chem., Int. Ed.* **2000**, *39*, 204. (g) Liu, J.; Gin, D. Y. *J. Am. Chem. Soc.* **2002**, *124*, 9789. (h) Storkey, C. M.; Win, A. L.; Hoberg, J. O. *Carbohydr. Res.* **2004**, *339*, 897–899. (i) Batchelor, R.; Hoberg, J. O. *Tetrahedron Lett.* **2003**, *44*, 9043–9045. (j) Hoberg, J. O. *J. Org. Chem.* **1997**, *62*, 6615–6618.

(12) Thiophenyl glycosides: (a) Boulineau, F. P.; Wei, A. *Org. Lett.* **2002**, *4*, 2281. (b) Gordon, D. M.; Danishefsky, S. J. *Carbohydr. Res.* **1990**, *206*, 361. Thioethyl glycosides: (c) Seeburger, P. H.; Eckhardt, M.; Gutteridge, C. E.; Danishefsky, S. J. *J. Am. Chem. Soc.* **1997**, *119*, 10064. Glycosyl phosphates: (d) Plante, O. J.; Andrade, R. B.; Seeburger, P. H. *Org. Lett.* **1999**, *1*, 211.

(13) (a) Allwein, S. P.; Cox, J. M.; Howard, B. E.; Johnson, H. W. B.; Rainier, J. D. *Tetrahedron* **2002**, *58*, 1997. (b) Postema, M. H. D.; Piper, J. L.; Liu, L.; Shen, J.; Faust, M.; Andreana, P. *J. Org. Chem.* **2003**, *68*, 4748. (c) Liu, L.; Postema, M. H. D. *J. Am. Chem. Soc.* **2001**, *123*, 8602.

(4) Pakulski, Z. *Pol. J. Chem.* **1996**, *70*, 667. An alternate route to mono-septanosides has also been observed recently. See: Enright, P. M.; Tosin, M.; Nieuwenhuizen, M.; Cronin, L.; Murphy, P. V. *J. Org. Chem.* **2002**, *67*, 3733.

(5) (a) Stevens, J. D. *Aust. J. Chem.* **1975**, *28*, 525. (b) Ng, C. J.; Stevens, J. D. *Carbohydr. Res.* **1996**, *284*, 241.

(6) (a) Driver, G. E.; Stevens, J. D. *Aust. J. Chem.* **1990**, *43*, 2063. (b) Ng, C. J.; Craig, D. C.; Stevens, J. D. *Carbohydr. Res.* **1996**, *284*, 249. (c) Tran, T. Q.; Stevens, J. D. *Aust. J. Chem.* **2002**, *55*, 171.

(7) Driver, G. E.; Stevens, J. D. *Carbohydr. Res.* **2001**, *334*, 81.

(8) McAuliffe, J. C.; Hindsgaul, O. *Synlett* **1998**, 307.

SCHEME 1

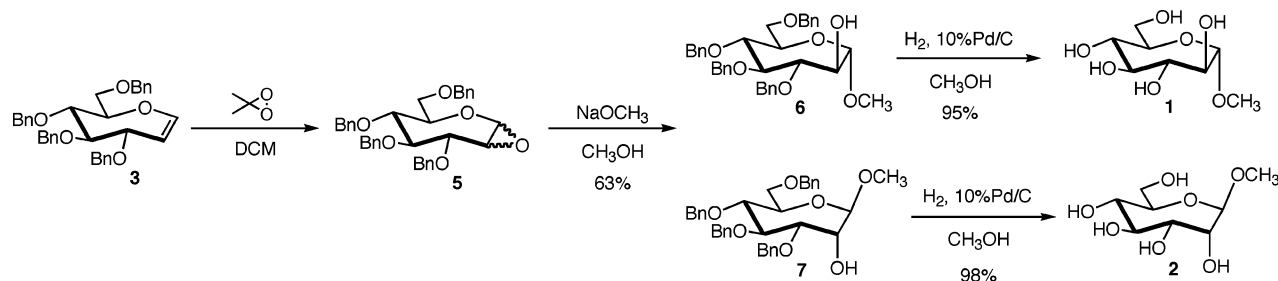
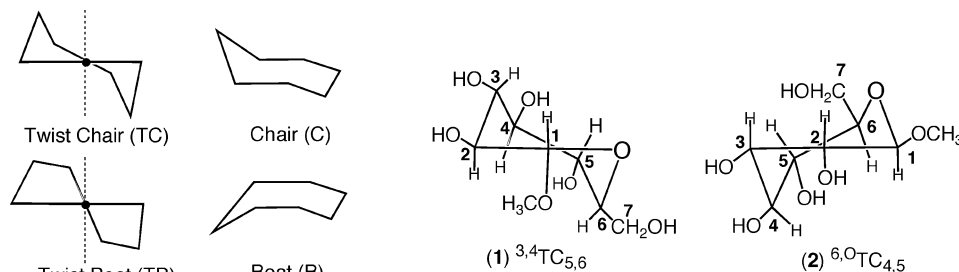


CHART 2



product analysis for the determination of the stereoselectivity in epoxidation of **3** was not possible. The prospect of using computational and spectroscopic methods in a synergistic manner to assign the stereochemistry of **1** and **2** gave us additional impetus to use a computational approach for determining the low-energy conformations of **1** and **2**.

The synthesis of **1** and **2** is shown in Scheme 1. Epoxidation of **3** using DMDO under standard conditions gave the corresponding anhydroseptanose **5**.¹⁴ The selectivity in epoxidation of **3** was much lower than that observed when using oxepine **4**; the origin of the deteriorated stereoselectivity is uncertain, but is being investigated. Nucleophilic opening of anhydroseptanose **5** using NaOCH₃/CH₃OH gave methyl glycosides **6** and **7** in 63% combined yield in a 1:3 (**6**:**7**) ratio. The product mixture was separated by column chromatography, and the benzyl groups were removed by hydrogenolysis for each isomer to give **1** and **2** in 95% and 98% yield, respectively. Based on the relative similarity of the NMR spectra and the paucity of reference data for *D*-glycero-*D*-septanosides, assignment of compound **1** versus **2** proved somewhat problematic. As a result, we approached the assignment of **1** and **2** through a comparison of computational and spectroscopic data.

B. General Conformational Analysis of Seven-Membered Rings. Conformational preferences of cycloheptane,¹⁵ oxepane,^{15d,16} and 1,3-/1,4-dioxepanes,^{15d,17}

among others,^{15c} have been described by modeling and spectroscopy. Low energy conformations of septanose carbohydrates have been reported in the solid state¹⁸ and in solution,¹⁹ but computational work on septanoses has not been described to date. Seven-membered ring systems in general show four low energy conformations; they are the twist-chair (TC), chair (C), twist-boat (TB), and boat (B) conformers (Chart 2) with the TC being most stable. For symmetric species such as cycloheptane, all of the TC conformers are energetically equivalent. Substituted rings of lower symmetry, however, have multiple and unique TC conformers; in fact, 14 unique TC conformers are possible with septanose carbohydrates. The nomenclature²⁰ for them is illustrated using the ^{3,4}TC_{5,6} conformer of **1** (Chart 2). For a given TC, three atoms define a molecular plane, and the remaining atoms lie above or below this plane. In the case of **1**, the ring oxygen, C₁, and C₂ are coplanar with each other, while C₃ and C₄ are above the plane and C₅ and C₆ are below the plane. An axis of pseudosymmetry, present in all of the TC conformers, is centered on C₁ of the ^{3,4}TC_{5,6} conformation. The atom and its substituents at this position are said to be isoclinal; because of the pseudosymmetry axis, isoclinal substituents experience the similar steric environments whether on the top or bottom face of the ring.^{15b,16a,21}

(14) Due to its relative lability, anhydroseptanose **5** was not isolated. It was routinely allowed to react with NaOCH₃/CH₃OH directly after its preparation. See the Supporting Information for the NMR spectra of **5**.

(15) (a) Bocian, D. F.; Pickett, H. M.; Rounds, T. C.; Strauss, H. L. *J. Am. Chem. Soc.* **1975**, *97*, 687. (b) Hendrickson, J. B. *J. Am. Chem. Soc.* **1967**, *89*, 7043. (c) Hendrickson, J. B. *J. Am. Chem. Soc.* **1967**, *89*, 7047. (d) Bocian, D. F.; Strauss, H. L. *J. Am. Chem. Soc.* **1977**, *99*, 2876. (e) Favini, G. *THEOCHEM* **1983**, *93*, 139.

(16) (a) Entrena, A.; Campos, J.; Gómez, J. A.; Gallo, M. A.; Espinosa, A. *J. Org. Chem.* **1997**, *62*, 337. (b) Espinosa, A.; Gallo, M. A.; Entrena, A.; Gómez, J. A. *J. Mol. Struct.* **1994**, *323*, 247.

(17) Espinosa, A.; Entrena, A.; Gallo, M. A.; Campos, J.; Domínguez, J. F.; Camacho, E.; Garrido, R. *J. Org. Chem.* **1990**, *55*, 6018

(18) (a) Bailey, C. J.; Craig, D. C.; Grainger, C. T.; James, V. J.; Stevens, J. D. *Carbohydr. Res.* **1996**, *284*, 265. (b) Craig, D. C.; Stevens, J. D. *Aust. J. Chem.* **1990**, *43*, 2083. (c) Foster, S. J. S. J.; James, V. J.; Stevens, J. D. *Acta Crystallogr.* **1989**, *C45*, 1329. (d) Wood, R. A.; James, V. J.; Rae, D. A.; Stevens, J. D.; Moore, F. H. *Aust. J. Chem.* **1983**, *36*, 2269. (e) Foster, S. J.; James, V. J.; Stevens, J. D. *Acta Crystallogr.* **1983**, *C39*, 610. (f) Choong, W.; McConnell, J. F.; Stephenson, N.; Stevens, J. D. *Aust. J. Chem.* **1980**, *33*, 979. (g) James, V. J.; Stevens, J. D. *Carbohydr. Res.* **1980**, *82*, 167. (h) McConnell, J. F.; Stevens, J. D. *J. Chem. Soc., Perkin Trans. 2* **1974**, 354. (i) Beale, J. P.; Stephenson, N. C.; Stevens, J. D. *Acta Crystallogr.* **1972**, *B28*, 3115. (j) Stevens, J. D.; Beale, J. P.; Stephenson, N. C. *J. Chem. Soc., Chem. Commun.* **1971**, *10*, 484.

(19) See refs 5–7 and also: Gonzalez, F. S.; Berenguel, A. V.; Molina, J. M. *Carbohydr. Res.* **1991**, *209*, 155.

(20) Stoddart, J. F. *Stereochemistry of Carbohydrates*; Wiley and Sons: New York, 1971.

An appropriately parametrized description of ring puckering provides an itinerary for the interconversion of low-energy conformations of flexible rings. For five-membered (furanose) rings, the phase angle (P) and puckering amplitude (τ_m) parameters define a pseudorotational itinerary (wheel) in which individual conformers are points on that wheel.²² For six-membered (pyranose) rings, the generalized description defined by Cremer and Pople correlates points on the surface of a sphere using a puckering amplitude (Q) and two angular variables, θ and ϕ .²³ The Pople treatment proposes that the “surface of a hypersphere in N-3 dimensions” will describe the conformations in higher rings. Bocian and Strauss have used similar variables (ρ , θ , ϕ_1 , ϕ_2) to describe conformations on the surface of a torus.¹⁵ A cross-section of the twist-chair (TC) to chair (C) surface shows the relative conformational energy as a function of the pseudorotational phase angle. A similar itinerary can be developed for the TB–B interconversion; however, in substituted systems, the TB and B conformers are high enough in energy that they are not readily populated. Increased steric interactions between substituents and the ring atoms in the TB and B conformers explain this general preference.¹⁶ The work reported here is concerned only with identifying the low-energy conformations of **1** and **2**; a description of their interconversion between alternative conformations will also require treatment of the above considerations.

Some general principles that govern septanose ring conformations can be derived from the systems noted above and from the structural information gathered on known examples of septanose carbohydrates. First, in each case, a TC conformation is almost exclusively the lowest energy conformation. Second, in the simpler systems, a distribution of multiple low-energy conformers of similar energies underscores their flexibility. Computational treatments of septanose carbohydrates are absent from the literature, but reported aqueous solution structures assign only one conformer.¹⁹ This apparent rigidity of monoseptanosides is therefore in contrast with the conformational flexibility that has been noted in the simpler seven-membered ring systems. Third, factors such as steric interactions between substituents, and electronic effects, such as the anomeric effect,^{24,25} can significantly influence which TC conformer is most stable. Of special note here are the steric factors associated with substituents on the isoclinal carbon. Several examples show that favored conformations will put large axial substituents (such as the OCH₃ group of the aglycon in septanoside **1**) into the isoclinal position so as to experi-

ence diminished steric interactions with the rest of the ring. Restricted rotation about the C₁–O₁ bond is also observed according to the exo-anomeric effect in calculated structures.²⁶ In total, the principles operative in determining preferred conformations of furanose and pyranose rings seem to be operative in the septanose series.

C. General Computational Methods. The Systematic Pseudo Monte Carlo search protocol available in MacroModel version 6.5²⁷ was used to generate 50 000 conformers of **1** and **2**. These structures were then optimized with the AMBER²⁸ force field using the dielectric constant of water; two Monte Carlo searches were performed for each compound. The first search merely varied the exocyclic dihedral angles and allowed the ring to adopt a suitable conformation while the second search varied both the exocyclic dihedral angles as well as the endocyclic dihedral angles within the septanose ring. Generating structural and conformational diversity was very important, and we utilized these Monte Carlo searches to guarantee a variety of conformations for further analysis. The first Monte Carlo search of **1**, using the dielectric constant of water, generated 437 unique conformations. The second search of **1** yielded 394 unique conformations. The first search of **2** yielded 499 unique conformations, while the second search yielded 341 conformations. Each conformer was given a unique number, starting from number 1 for the calculated global minimum at the AMBER level and then increasing up the energy manifold. Conformations from the second search have been denoted by an asterisk in the subsequent tables.

In the case of **1**, the conformations within 4 kcal/mol of the global minimum predicted by the AMBER force field (approximately 40 conformers) were then further optimized using the Minnesota Gaussian Solvation Model (MN-GSM)²⁹ at the SM5.42/HF/6-31G* level using parameters for water as a solvent. These and subsequent calculations were performed with Gaussian 98.³⁰ In the case of **2**, conformations (approximately 40 conformers) within 5 kcal/mol were carried through for optimization with MN-GSM because there were fewer conformations within 4 kcal/mol than there were for **1**. The geometry

(21) Hendrickson, J. B. *J. Am. Chem. Soc.* **1964**, *86*, 4854.

(22) Altona, C.; Sundaralingam, M. *J. Am. Chem. Soc.* **1972**, *94*, 8205.

(23) Cremer, D.; Pople, J. A. *J. Am. Chem. Soc.* **1975**, *97*, 1354.

(24) (a) Kirby, A. J. *The Anomeric Effect and Related Stereoelectronic Effects at Oxygen*; Springer-Verlag: New York, 1983. (b) Szarek, W. A.; Horton, D.; Eds. *Anomeric Effect. Origins and Consequences*; ACS Symposia Series 87; American Chemical Society: Washington, DC, 1979. (c) Deslongchamps, P. *Stereoelectronic Effects in Organic Chemistry*; Wiley: New York, 1983. (d) Thatcher, G. R. J., Ed. *The Anomeric Effect and Associated Electronic Effects in Organic Chemistry*; ACS Symposia Series 539; American Chemical Society: Washington, DC, 1993.

(25) For discussion of the anomeric effect in seven-membered rings see ref 16a and: (a) Désilets, S.; St-Jacques, M. *J. Am. Chem. Soc.* **1987**, *109*, 1641. (b) Désilets, S.; St-Jacques, M. *Can. J. Chem.* **1992**, *70*, 2650.

(26) (a) Lemieux, R. U.; Pavis, A. A.; Martin, J. C.; Watanabe, K. *H. Can. J. Chem.* **1969**, *47*, 427. (b) Booth, H.; Khedahair, K. A.; Readshow, S. A. *Tetrahedron* **1987**, *43*, 4699.

(27) (a) MacroModel V6.5: Mohamadi, F.; Richards, N. G. J.; Guida, W. C.; Liskamp, R.; Lipton, M.; Caulfield, C.; Chang, G.; Hendrickson, T.; Still, W. C. *J. Comput. Chem.* **1990**, *11*, 440. (b) Goodman, J.; Still, W. C. *J. Comput. Chem.* **1991**, *12*, 1110.

(28) (a) Homans, S. W. *Biochemistry* **1990**, *29*, 9112. (b) Weiner, S. J.; Kollman, P. A.; Case, D. A.; Singh, U. C.; Ghio, C.; Alagona, C.; Profeta, S., Jr.; Weiner, P. *J. Am. Chem. Soc.* **1984**, *106*, 765. (c) Cornell, W. D.; Cieplak, P.; Bayly, C. I.; Gould, I. R.; Merz, K. M., Jr.; Ferguson, D. M.; Spellmeyer, D. C.; Fox, T.; Caldwell, J. W.; Kollman, P. A. *J. Am. Chem. Soc.* **1995**, *117*, 5179. (d) Senderowitz, H.; Parish, C.; Still, W. C. *J. Am. Chem. Soc.* **1996**, *118*, 2078. (e) Senderowitz, H.; Still, W. C. *J. Org. Chem.* **1997**, *62*, 1427. (f) For an excellent evaluation of the AMBER force field for carbohydrates, see Table 7 in: Barrows, S. E.; Storer, J. W.; Cramer, C. J.; French, A. D.; Truhlar, D. G. *J. Comput. Chem.* **1998**, *19*, 1111.

(29) (a) Xidos, J. D.; Li, J.; Hawkins G. D.; Liotard, D. A.; Cramer, C. J.; Truhlar, D. G.; Frisch, M. J. *MN-GSM*, version 99.2; University of Minnesota: Minneapolis, MN 55455. (b) Li, J.; Zhu, T.; Cramer, C. J.; Truhlar, D. G. *J. Phys. Chem. A* **1998**, *102*, 1820. (c) Li, J.; Hawkins, G. D.; Cramer, C. J.; Truhlar, D. G. *Chem. Phys. Lett.* **1998**, *288*, 293. (d) Zhu, T.; Li, J.; Hawkins, G. D.; Cramer, C. J.; Truhlar, D. G. *J. Chem. Phys.* **1998**, *109*, 9117. (e) Li, J.; Zhu, T.; Hawkins, G. D.; Winget, P.; Liotard, D. A.; Cramer, C. J.; Truhlar, D. G. *Theor. Chem. Acc.* **1999**, *103*.

optimizations for **2** were also performed at the SM5.42/HF/6-31G* level of theory with water as the solvent. Gas-phase single-point energies were obtained at the HF/6-31G* and B3LYP/6-31+G** levels of theory.

With these data on hand, the $E_{\text{B3LYP/6-31+G**/SM5.42/HF/6-31G*}(\text{solution})}$ (referred to as the DFT/MN-GSM energy) was determined from the following equation:³¹

$$\Delta G_{\text{solvation}} = E_{\text{SM5.42/X/6-31G*}} - E_{\text{HF/6-31G*}(\text{gas})} \\ E_{\text{B3LYP/6-31+G**/SM5.42/HF/6-31G*}(\text{solution})} = \\ E_{\text{B3LYP/6-31+G**/SM5.42/HF/6-31G*}(\text{gas})} + \Delta G_{\text{solvation}}$$

Many of the conformations, upon optimization, generated duplicate structures. The result of these optimizations at the SM5.42/HF/6-31G* level was that 16 unique conformations were found within 5 kcal/mol of the global minimum for compound **1**, and 19 unique conformations were obtained for compound **2** within 5 kcal/mol of its global minimum. The energies of these conformations were then refined to determine their contribution to the overall Boltzmann distribution. A vibrational frequency analysis was performed for each of the conformations that contributed to greater than 2% of the Boltzmann distribution in order to confirm that each was, in fact, a true minimum.

Monte Carlo searches were also performed for each of the septanosides and optimized in the absence of a dielectric field with the AMBER force field. All conformers within 5 kcal/mol of the global minimum (according to the AMBER force field) were then optimized at the HF/6-31G* level of theory in the gas phase. Vibrational frequency analysis was performed for each of the conformers to verify that they were true minima. The bottom-of-the-well energies at the HF/6-31G* level of theory were then used to calculate the contribution of each of these conformers to the Boltzmann distribution.

NMR coupling constants were determined for each of the various conformations from the SM5.42/HF/6-31G* optimizations using the deMon-NMR software package.³² The Perdew and Wang exchange and Perdew correlation

functional with the IGLO III basis set were used in all of these calculations.³³ These calculated one-bond and three-bond coupling constants were then compared with the experimental NMR coupling constants to aid in the determination of the conformation of the septanose ring.

D. Computational Results. 1. Monte Carlo Results for Septanoside 1. The Monte Carlo searches for **1** resulted in approximately 800 conformations that were shown to cover a very wide variety of internal dihedral angles for the septanose ring (see Supporting Information for details); therefore, extensive and diverse coverage of the conformational space of this structure was obtained by the Monte Carlo approach.

Assignment of the conformation of the ring was made by visual inspection of the conformations within 4 kcal/mol of the global minimum, according to the AMBER force field (see the Supporting Information), and each conformer was given a unique number, starting from number 1 for the calculated global minimum at the AMBER level. The majority of the lowest energy conformations, especially those within 2 kcal/mol of the global minimum, adopted a ^{3,4}TC_{5,6} conformation. The next most abundant conformation was found to be a ^{1,2}TC_{3,4} conformation. Although a couple of chair structures as well as one other type of twist-chair structure were found in these lowest energy conformations, there appears to be much less conformational flexibility for the septanose ring than might have been originally anticipated. In fact, the Monte Carlo search does adequately generate conformational diversity for the various conformations that the septanose ring may adopt, but the majority of these conformations appear to comprise very high energy structures. The global minimum, according to the AMBER force field, for the α anomer of **1** was determined to be a ^{3,4}TC_{5,6} conformation (Chart 2). Each individual AMBER conformational search predicted the exact same structure as the global minimum. The major difference among the conformations within 4 kcal/mol of this global minimum is due to the orientation of the exocyclic OH bonds as well as the C₆–C₇ dihedral angle. Based on the O–H...O distances and angles, these interactions appear to be apparent hydrogen bonds between the exocyclic OH groups.³⁴ All of the low energy conformations appear to adopt conformations that allow for a high degree of hydrogen bonding among the exocyclic OH bonds, even with the inclusion of the dielectric constant of water for the simulation. Indeed, computational studies have shown that intramolecular hydrogen bonding is diminished, but not eliminated, in ethylene glycol³⁵ or glycerol³⁶ upon inclusion of aqueous solvation.

2. MN-GSM Results for Septanoside 1. The conformations within 4 kcal/mol of the global minimum, according to the AMBER force field, were then fully optimized at the SM5.42/HF/6-31G* level of theory (Table

(30) Frisch, M. J.; Trucks, G. W.; Schlegel, H. B.; Scuseria, G. E.; Robb, M. A.; Cheeseman, J. R.; Zakrzewski, V. G.; Montgomery, J. A., Jr.; Stratmann, R. E.; Burant, J. C.; Dapprich, S.; Millam, J. M.; Daniels, A. D.; Kudin, K. N.; Strain, M. C.; Farkas, O.; Tomasi, J.; Barone, V.; Cossi, M.; Cammi, R.; Mennucci, B.; Pomelli, C.; Adamo, C.; Clifford, S.; Ochterski, J.; Petersson, G. A.; Ayala, P. Y.; Cui, Q.; Morokuma, K.; Malick, D. K.; Rabuck, A. D.; Raghavachari, K.; Foresman, J. B.; Cioslowski, J.; Ortiz, J. V.; Stefanov, B. B.; Liu, G.; Liashenko, A.; Piskorz, P.; Komaromi, I.; Gomperts, R.; Martin, R. L.; Fox, D. J.; Keith, T.; Al-Laham, M. A.; Peng, C. Y.; Nanayakkara, A.; Gonzalez, C.; Challacombe, M.; Gill, P. M. W.; Johnson, B.; Chen, W.; Wong, M. W.; Andres, J. L.; Gonzalez, C.; Head-Gordon, M.; Replogle, E. S.; Pople, J. A. *Gaussian 98, Revision A.7*, Gaussian, Inc.; Pittsburgh, PA, 1998.

(31) Houseknecht, J. B.; McCarren, P. R.; Lowary, T. L.; Hadad, C. M. *J. Am. Chem. Soc.* **2001**, *123*, 8811.

(32) (a) St-Amant, A.; Salahub, D. R. *Chem. Phys. Lett.* **1990**, *169*, 387. (b) Casida, M. E.; Daul, C.; Goursot, A.; Koester, A.; Pettersson, L.; Proynov, E.; St-Amant, A.; Salahub, D. R.; Duarte, H.; Godbout, N.; Guan, J.; Jamorski, C.; Leboeuf, M.; Malkin, V.; Malkina, O.; Sim, F.; Vela, A. *deMon-KS, version 3.4*; deMon Software, 1996. (c) Malkin, V. G.; Malkina, O. L.; Salahub, D. R. *Chem. Phys. Lett.* **1994**, *221*, 91. (d) Malkina, O. L.; Salahub, D. R.; Malkin, V. G. *J. Chem. Phys.* **1996**, *105*, 8793. (e) Salahub, D. R.; Fournier, R.; Mlynarski, P.; Papai, I.; St-Amant, A.; Uskio, J. In *Density Functional Methods in Chemistry*; Labanowski, J. K.; Anzelm, J. W., Eds.; Springer: New York, 1991; p 77. (f) Malkin, V. G.; Malkina, O. L.; Casida, M. E.; Salahub, D. R. *J. Am. Chem. Soc.* **1994**, *116*, 5898.

(33) (a) Perdew, J. P.; Wang, Y. *Phys. Rev. B* **1986**, *33*, 8800. (b) Perdew, J. P. *Phys. Rev. B* **1986**, *33*, 8822. (c) Perdew, J. P. *Phys. Rev. B* **1986**, *34*, 7406.

(34) The classification of these O–H...O interactions as hydrogen bonds is based on the calculated bond distances and angles. Topologically, hydrogen bonds can be characterized based on minima in the overall electron density as demonstrated by: Klein, R. A. *J. Am. Chem. Soc.* **2002**, *124*, 13931.

(35) Cramer, C. J.; Truhlar, D. G. *J. Am. Chem. Soc.* **1994**, *116*, 3892.

(36) Callam, C. S.; Singer, S. J.; Lowary, T. L.; Hadad, C. M. *J. Am. Chem. Soc.* **2001**, *123*, 11743.

TABLE 1. Calculated Conformational Distribution for the α Septanoside Anomer (1)^a

conformer ^b	E_{rel} AMBER	E_{rel} SM5.42/HF/6-31G*	E_{rel} B3LYP/6-31+G**// SM5.42/HF/6-31G* (solution)	Boltzmann contribution ^c (%)	ring conformation	C ₆ –C ₇ rotamer
36	3.67	0.00	0.00	73.78	^{3,4} TC _{5,6}	tg
12	1.75	1.25	1.43	6.60	^{3,4} TC _{5,6}	gt
1	0.00	1.97	1.47	6.11	^{3,4} TC _{5,6}	gt
3	0.54	1.84	1.61	4.86	^{3,4} TC _{5,6}	gg
22	2.38	1.91	1.79	3.59	^{3,4} TC _{5,6}	gt
5	0.91	2.49	2.04	2.36	^{3,4} TC _{5,6}	gt
9*	1.06	2.72	2.18	1.83	^{3,4} TC _{5,6}	gt
13	1.77	3.20	3.20	0.33	^{1,2} TC _{3,4}	gg
52*	3.97	4.49	3.67	0.15	^{1,2} TC _{3,4}	gt
4	0.79	4.49	3.68	0.15	^{1,2} TC _{3,4}	gt
30	3.39	4.30	4.07	0.08	^{3,4} TC _{5,6}	gg
23	2.58	4.80	4.25	0.06	^{3,4} TC _{5,6}	gg
37*	3.50	4.72	4.59	0.03	^{3,4} TC _{5,6}	gg
26*	1.85	5.47	4.68	0.03	^{3,4} TC _{5,6}	gg
18	1.98	5.68	4.95	0.02	^{1,2} TC _{3,4}	gg
20	2.20	5.70	4.97	0.02	^{3,4} TC _{5,6}	gt
17	1.80	5.88	4.99	0.02	^{3,4} TC _{5,6}	gg

^a Relative energies for each conformer, at each level of theory, are in kcal/mol. ^b Conformers from the second Monte Carlo search (as unique structures) are denoted with an asterisk. ^c The Boltzmann contribution, as a percentage, is determined based on the relative energies calculated at the B3LYP/6-31+G**//SM5.42/HF/6-31G* (solution) level of theory.

1). One result of this optimization sequence became readily apparent. At the SM5.42/HF/6-31G* level, conformer 36 from the original Monte Carlo search, and not conformer 1, became the global minimum. We, therefore, set about to determine the origin of this discrepancy between the two theoretical methods. Comparison of the optimized geometries at the AMBER and SM5.42/HF/6-31G* levels demonstrated that there was not a significant change made to the geometry upon optimization at the higher level of theory. Therefore, we postulated that the energetic results by each theoretical method was more critical. To verify this hypothesis, gas-phase, single-point energies were calculated at the HF/6-31G* and B3LYP/6-31G* levels of theory using the AMBER-optimized geometries. The comparison of these single-point energies to those calculated for the SM5.42/HF/6-31G*-optimized geometries demonstrated that the AMBER force field was fairly poor at determining the correct order of the lowest energy conformations (see the Supporting Information for details).

Little difference was observed between the AMBER-optimized geometries and the SM5.42/HF/6-31G*-optimized geometries; however, enough change was observed such that the total number of unique conformations found at the end of the MN-GSM optimization regimen was 16 (one structure was found to be a transition state and not a true minimum). Many of the conformations from the two Monte Carlo searches optimized to the same structures. The global minimum at the SM5.42/HF/6-31G* level of theory was found to be a ^{3,4}TC_{5,6} conformation. Both AMBER and SM5.42/HF/6-31G* predict a global minimum wherein all of the OH bonds form a cyclic hydrogen-bonding array in which each OH unit is hydrogen bonded to the next (Figure 1). The difference between the global minima predicted lies in the rotamer orientation about the C₆–C₇ bond. SM5.42/HF/6-31G* predicts a global minimum in which the C₆–C₇ bond lies in a tg orientation (Chart 3) so as to allow the hydroxyl group on C₇ to hydrogen bond to the hydroxyl group on C₅. The AMBER force field predicted this C₆–C₇ rotamer to be gt, allowing for hydrogen bonding with the ring oxygen rather than O₅. Conformer 12, which has a

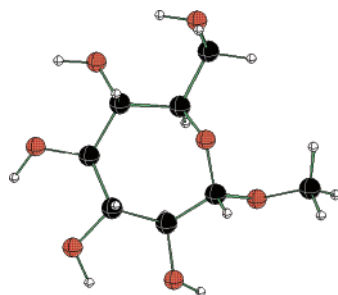
relative energy (according to SM5.42/HF/6-31G*) just between that of 36 and 1, has a nearly identical structure to that of conformer 1 except for the orientation about the C₆–C₇ bond.

Calculation of the contributions that each conformer makes to the Boltzmann distribution demonstrated some interesting details. The SM5.42/HF/6-31G* calculations predict that the global minimum (conformation 36) would comprise approximately 73% of the Boltzmann distribution. Therefore, this conformer is very highly favored to the exclusion of nearly all others. It would appear from these calculations that the α anomer of **1** should exist almost exclusively in the ^{3,4}TC_{5,6} conformation in water. The C₆–C₇ rotamer should also exist preferentially in the tg conformation. All other conformations should be very unfavorable and make much less contribution to the overall properties of this septanose species.

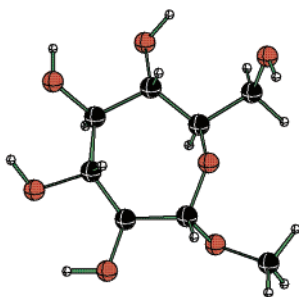
3. Gas-Phase HF/6-31G* Results for Septanoside

1. The conformations from the gas-phase Monte Carlo search within 5 kcal/mol were optimized at the HF/6-31G* level of theory. The optimization process resulted in 20 unique conformations, spanning an energy range of approximately 7 kcal/mol. The results of these calculations are presented in Table 2. As in the case of the MN-GSM-optimized geometries, the ring conformations were found to be overwhelmingly in the ^{3,4}TC_{5,6} conformation with the ^{1,2}TC_{3,4} being the next most common conformation. Conformer 17 from the original Monte Carlo search was found to be the global minimum with a ring conformation of ^{3,4}TC_{5,6} and a tg C₆–C₇ rotamer. This is the same global minimum as found at the MN-GSM level. The Boltzmann contribution of this conformer also correlates very well with that found using the solvation model. All of the conformers within 4 kcal/mol of the global minimum were identical to those found using the SM5.42/HF/6-31G* level of theory. Figure 2 depicts the structures of the lowest energy conformers. The Boltzmann contributions of each of these conformers was, likewise, very comparable to those calculated in the presence of water as the solvent.

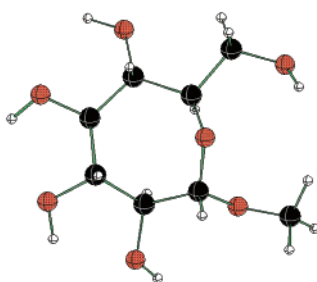
4. Monte Carlo Results for Septanoside 2. Monte Carlo searches for **2** resulted in approximately 850 total



Conformer 36 (${}^3,4\text{TC}_{5,6}$)
 AMBER $E_{\text{rel}} = 3.67$ kcal/mol
 DFT MN-GSM $E_{\text{rel}} = 0.00$ kcal/mol
 Boltzmann Contribution = 73.78%



Conformer 12 (${}^3,4\text{TC}_{5,6}$)
 AMBER $E_{\text{rel}} = 1.75$ kcal/mol
 DFT MN-GSM $E_{\text{rel}} = 1.43$ kcal/mol
 Boltzmann Contribution = 6.60%

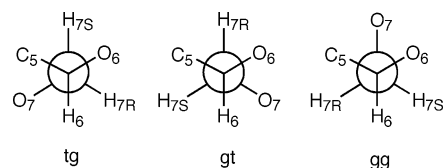


Conformer 1 (${}^3,4\text{TC}_{5,6}$)
 AMBER $E_{\text{rel}} = 0.00$ kcal/mol
 DFT MN-GSM $E_{\text{rel}} = 1.47$ kcal/mol
 Boltzmann Contribution = 6.11%

FIGURE 1. Low energy conformers of α anomer (**1**). The conformer number, ring conformation, relative energies at the AMBER and B3LYP/6-31+G**//SM5.42/HF/6-31G* levels of theory, as well as contribution to the Boltzmann distribution are also shown.

conformations. All structures within 5 kcal/mol were examined and visually assigned a configuration (see the Supporting Information). It was observed that these low energy structures consisted mainly of septanose rings in the ${}^6,0\text{TC}_{4,5}$ conformation (Chart 2). The next most prevalent conformer in these structures is the ${}^1,2\text{TC}_{3,4}$ conformation. As in the case of the α anomer, these conformations make up the bulk of the low-lying conformations with a couple of other twist-chair and chair

CHART 3



conformations interspersed. The global minimum for **2**, according to the AMBER force field, was found to be a ${}^6,0\text{TC}_{4,5}$ conformer with all of the exocyclic hydroxyl groups arranged in a similar cyclic hydrogen bonding array as was observed for the α anomer (**1**). It should be noted that, again, all of these low-lying conformations exhibit the same hydrogen-bonding pattern. There are some differences in the conformation of the ring and in the $\text{C}_6\text{--C}_7$ rotamer that give rise to the number of unique conformers. In the case of **2**, as noted in **1**, both AMBER conformational searches predicted the same global minimum, and many of the same conformers are within 5 kcal/mol.

It is noteworthy that the ${}^1,2\text{TC}_{3,4}$ was represented in the Monte Carlo simulations of both **1** and **2**. This conformation puts C_6 , and subsequently the exocyclic hydroxymethyl group, into the isoclinal position. Based on the preference for large groups to occupy the isoclinal position, this result is not surprising. The fact that the ${}^1,2\text{TC}_{3,4}$ conformer is energetically accessible (~ 3.5 kcal/mol higher in energy for **1** and **2**) from the global minimum suggests that the ${}^1,2\text{TC}_{3,4}$ conformer may be preferred if the size of the C_6 substituent is increased (by glycosylation, for example).

5. MN-GSM Results for Septanoside 2. All structures within 5 kcal/mol of the global minimum of **2** were then optimized using the SM5.42/HF/6-31G* approach (Table 3). Many structures were found to be identical after this optimization and resulted in a total of 19 unique conformers. For the case of **2**, the AMBER force field performed slightly better at predicting the global minimum than it had for **1**. The global minimum was found to be conformer 40* (obtained from the second Monte Carlo search). For the β anomer **2**, conformer 1 was found to be very close in energy to conformer 40* (approximately 0.05 kcal/mol), considerably closer than the difference in energy between conformers 1 and 36 for the α anomer **1**.

The global minimum (conformer 40*) at the SM5.42/HF/6-31G* level has the same ring conformation of the septanose ring as conformer 1, the global minimum at the AMBER level. The only difference between the two structures is the orientation of the $\text{C}_6\text{--C}_7$ bond (Figure 3). Once again, AMBER favors the gt orientation whereas SM5.42/HF/6-31G* favors the tg orientation (Chart 3). As in the case of the α anomer (**1**), the difference is due to the relative orientations of hydrogen bonds with the ring oxygen and O_5 , respectively. Apparently, AMBER dramatically overestimates the energetic difference between these two orientations.

Three additional conformers were found to lie within 1 kcal/mol of the global minimum (conformers 3, 9, and 26*). These three conformers were virtually identical by visual inspection, and they differed only slightly in the dihedral angles within the ring itself. All three are also ${}^6,0\text{TC}_{4,5}$ conformations of the ring, much like conformers

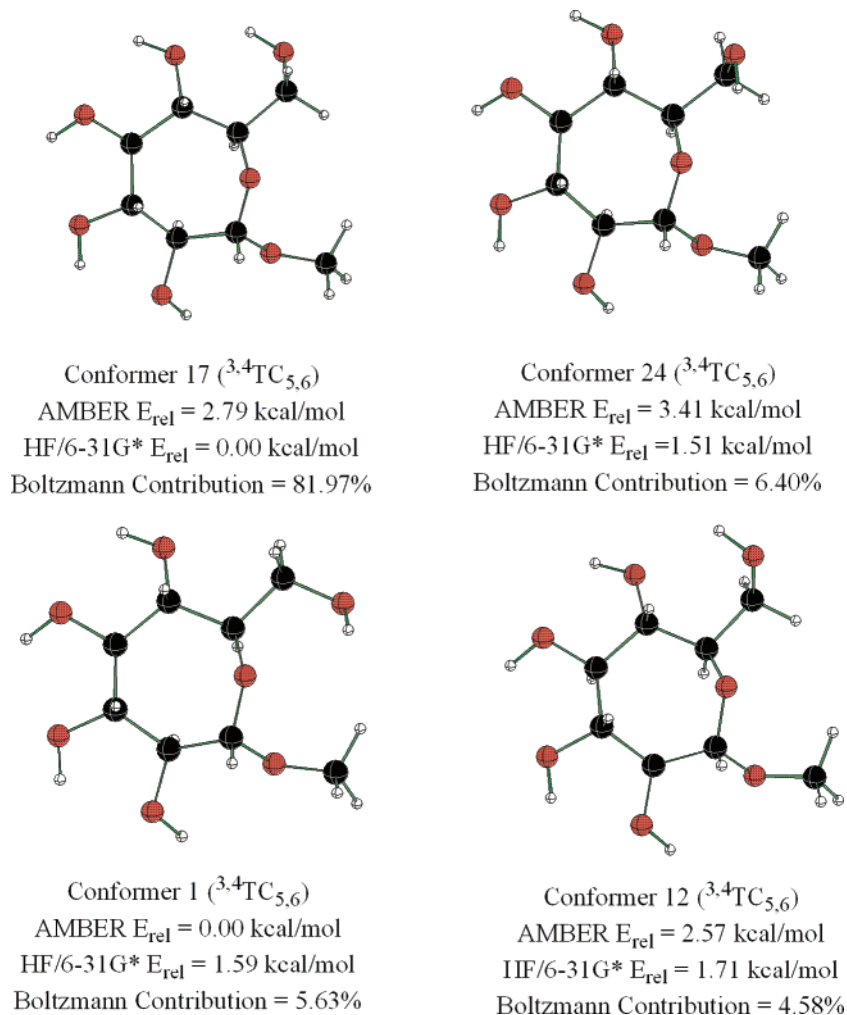


FIGURE 2. Low energy conformers of α anomer (**1**) in the gas phase (HF/6-31G*). The conformer number, ring conformation, relative energies at the AMBER and HF/6-31G* levels of theory as well as the contribution to the Boltzmann distribution are shown.

40* and **1**. These conformers lie approximately 0.5 kcal/mol above the global minimum. They differ from conformers 40* and **1** mainly in the $\text{C}_6\text{--C}_7$ orientation (Figure 2). Conformers 3, 9, and 26* are gg rotamers with the hydroxyl group pointed in such a way as to allow for hydrogen-bonding interactions with the ring oxygen.

Calculations were made to determine the contributions that each of these 19 conformers would make to the Boltzmann distribution. It was found that conformers 40*, **1**, 3, 9, and 26* made up the bulk (94%) of the Boltzmann distribution. Although there is expected to be very little conformational flexibility of the ring itself (it should be predominantly fixed in the ${}^{6,0}\text{TC}_{4,5}$ conformation), there is a significant amount of flexibility to be expected for the orientation about the $\text{C}_6\text{--C}_7$ bond. This is in stark contrast to the calculated results for the α anomer **1** in which the tg rotamer was predicted to be favored by at least 1.25 kcal/mol over the other rotamers. For the β anomer **2**, there is only a maximum of 0.5 kcal/mol separating the rotamers, as predicted at the SM5.42/HF/6-31G* level.

6. Gas-Phase HF/6-31G* Results for Septanoside 2. The conformations from the gas-phase Monte Carlo search for **2** within 5 kcal/mol were optimized at the HF/

6-31G* level of theory. The optimization process resulted in 22 unique conformations, spanning an energy range of approximately 7 kcal/mol. The results of these calculations are given in Table 4. The results of the calculations are, again, extremely similar to those of the MN-GSM optimization sequence. The two lowest energy conformers have a ring conformation of ${}^{6,0}\text{TC}_{4,5}$ and correspond to the gt and tg $\text{C}_6\text{--C}_7$ rotamers. The lowest energy conformer is the gt rotamer with a Boltzmann contribution of 33%. The tg rotamer is only 0.07 kcal/mol higher in energy than the global minimum and contributes 29% to the overall Boltzmann distribution. Both of the conformers are nearly identical to those found at the MN-GSM level. Figure 4 depicts the structures of the lowest energy conformers that contribute most significantly to the Boltzmann distribution. Most of the conformers are identical to those found under MN-GSM with the exception of conformers 49 and 42. Conformer 49 has a ring conformation of ${}^{4,5}\text{TC}_{2,3}$ and conformer 42 has a ring conformation of ${}^{5,6}\text{TC}_{0,1}$. Both of these ring conformations were found not to exist in the lowest energy conformers found at the MN-GSM level and represent about 13% of the Boltzmann distribution. With the exception of these

TABLE 2. Calculated Conformational Distribution for the α Septanoside Anomer (**1**) in the Gas Phase^a

conformer	E_{rel} AMBER	E_{rel} HF/6-31G*	ring conformation	C ₆ -C ₇ rotamer	Boltzmann contribution ^b (%)
17	2.79	0.00	^{3,4} TC _{5,6}	tg	81.97
24	3.41	1.51	^{3,4} TC _{5,6}	gg	6.40
1	0.00	1.59	^{3,4} TC _{5,6}	gt	5.63
12	2.57	1.71	^{3,4} TC _{5,6}	gg	4.58
7	1.36	2.55	^{3,4} TC _{5,6}	gt	1.11
6	1.34	3.31	^{1,2} TC _{3,4}	gg	0.31
36	4.02	3.38	^{3,4} TC _{5,6}	gg	0.27
3	0.90	4.35	^{1,2} TC _{3,4}	gt	0.05
22	3.14	5.30	^{1,2} TC _{3,4}	gt	0.01
28	3.55	5.44	^{3,4} TC _{5,6}	gg	0.01
37	4.09	5.53	^{3,4} TC _{5,6}	gt	0.01
8	2.27	5.60	^{3,4} TC _{5,6}	gt	0.01
44	5.03	5.67	^{3,4} TC _{5,6}	gg	0.01
35	3.94	5.99	^{3,4} TC _{5,6}	gt	0.00
40	4.15	6.22	^{3,4} TC _{5,6}	gt	0.00
39	4.15	6.56	^{3,4} TC _{5,6}	gt	0.00
23	3.30	6.84	^{1,2} TC _{3,4}	gg	0.00
15	2.64	6.93	^{1,2} TC _{3,4}	gt	0.00
31	3.72	7.10	^{3,4} TC _{5,6}	gt	0.00
41	4.28	7.24	^{1,2} TC _{3,4}	gg	0.00

^a Relative energies for each conformer, at each level of theory, are in kcal/mol. ^b The Boltzmann contribution, as a percentage, is determined based on the relative energies calculated at the HF/6-31G* level of theory.

TABLE 3. Calculated Conformational Distribution for the β Septanoside Anomer (**2**)^a

conformer ^b	E_{rel} AMBER	E_{rel} SM5.42/HF/6-31G*	E_{rel} B3LYP/6-31+G** // SM5.42/HF/6-31G* (solution)	Boltzmann contribution ^c (%)	ring conformation	C ₆ -C ₇ rotamer
40*	4.77	0.00	0.00	29.83	^{6,0} TC _{4,5}	tg
1	0.00	0.12	0.05	27.21	^{6,0} TC _{4,5}	gt
3	1.02	0.50	0.50	12.84	^{6,0} TC _{4,5}	gg
9	2.11	0.58	0.52	12.45	^{6,0} TC _{4,5}	gg
26*	3.66	0.55	0.54	11.94	^{6,0} TC _{4,5}	gg
4	1.66	1.82	1.60	1.99	^{6,0} TC _{4,5}	gt
8*	1.78	2.01	1.77	1.51	^{6,0} TC _{4,5}	gt
49*	4.88	1.55	2.02	0.98	⁵ C _{1,2}	gg
2	0.64	2.37	2.31	0.60	^{5,6} TC _{0,1}	gt
27*	3.66	3.59	3.14	0.15	^{6,0} TC _{4,5}	gg
11	2.41	3.58	3.32	0.11	^{6,0} TC _{4,5}	gt
6	1.78	2.70	3.46	0.09	^{1,2} TC _{3,4}	gt
11*	1.99	3.32	3.47	0.09	^{6,0} TC _{4,5}	gt
14	2.88	3.46	3.60	0.07	^{6,0} TC _{4,5}	gg
10*	1.98	3.76	3.73	0.05	^{6,0} TC _{4,5}	gt
7	2.01	4.01	3.80	0.05	^{6,0} TC _{4,5}	gt
17	3.02	4.15	4.33	0.02	^{6,0} TC _{4,5}	gg
37*	4.56	3.82	4.47	0.02	^{3,4} TC _{5,6}	gt
13	2.59	5.15	4.74	0.01	^{5,6} TC _{0,1}	gt

^a Relative energies for each conformer, at each level of theory, are in kcal/mol. ^b Conformers from the second Monte Carlo search (as unique structures) are denoted with an asterisk. ^c The Boltzmann contribution, as a percentage, is determined based on the relative energies calculated at the B3LYP/6-31+G**//SM5.42/HF/6-31G* level of theory.

two conformers, the gas-phase results are nearly identical to those under the solvation model.

7. Calculation of Theoretical NMR Coupling Constants. NMR coupling constants were calculated for each of the protons on the septanose ring. The coupling constants were determined for each of the 17 unique conformers determined for **1** and for each of the 19 unique conformers of **2**. These values were then weighted according to the Boltzmann distribution of these conformers at the B3LYP/6-31+G**//SM5.42/HF/6-31G* level and summed to yield overall coupling constants for the α and β anomers (**1** and **2**, respectively). The results of the calculated coupling constants of the ring hydrogens are summarized in Table 5.

Of particular note are the differences between the α and β anomers. Both have very similar values for the ³J_{1,2}, ³J_{4,5}, and ³J_{5,6} coupling constants. The difference

between **1** and **2** lies in the ³J_{2,3} and ³J_{3,4} coupling constants. The α anomer (**1**) should have a ³J_{2,3} value of approximately 8.9 Hz and a ³J_{3,4} value of approximately 7.5 Hz. The β anomer, **2**, in contrast, should have a ³J_{2,3} value of approximately 5.4 Hz and a ³J_{3,4} value of approximately 9.1 Hz. It appears that these coupling constants are particularly indicative of the differences between the ^{3,4}TC_{5,6} conformation of the α anomer and the ^{6,0}TC_{4,5} conformation of the β anomer. *Thus, it should be very straightforward to assign the structures by NMR.* In fact, the values of these coupling constants are in good agreement with the experimental observations, and the largest deviations are observed for the ³J_{2,3} coupling in **2** and the ³J_{5,6} coupling in **1**. In general, the coupling constants are within approximately 1 Hz of the experimental values, and there does not appear to be a consistent trend of the deMon-NMR calculated coupling

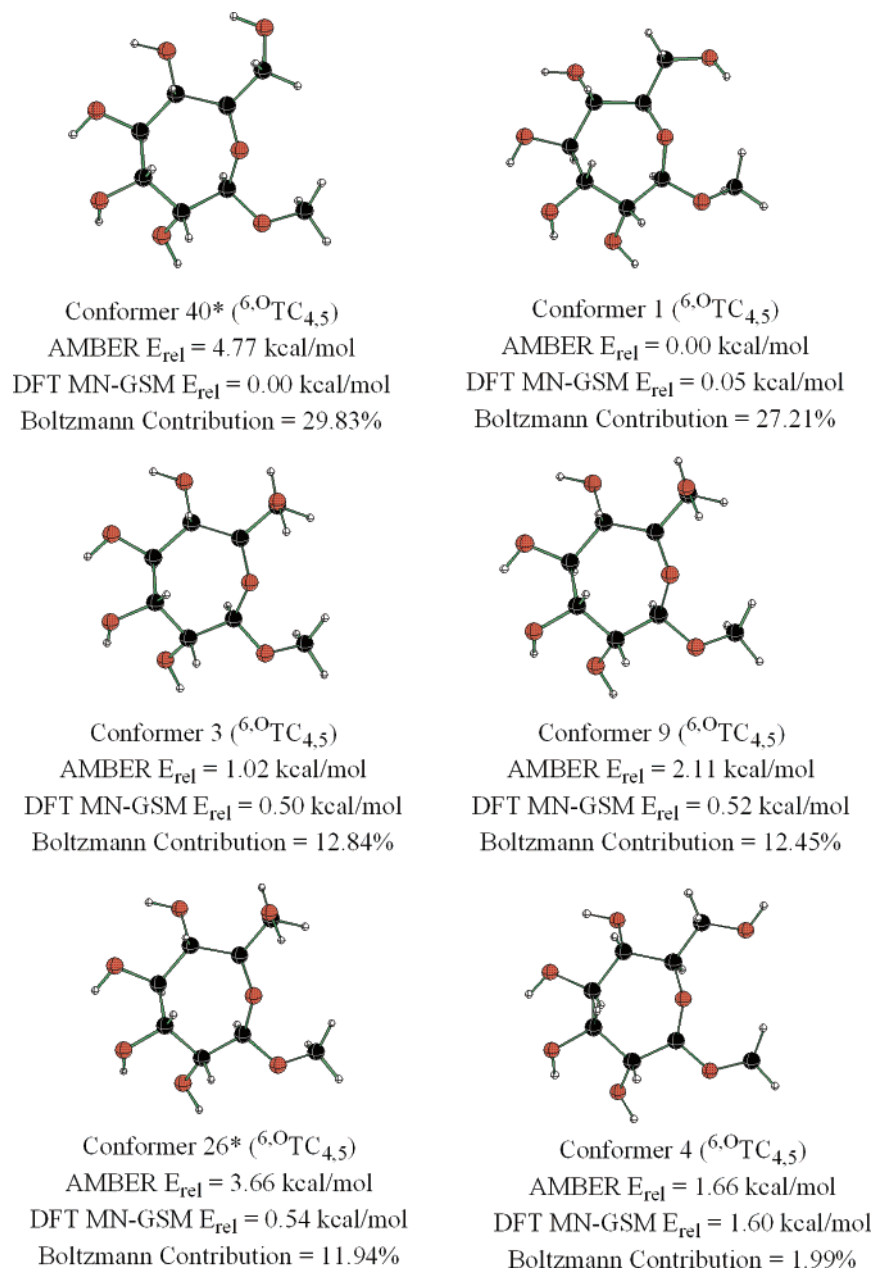


FIGURE 3. Low energy conformers for β anomer **2**. The conformer number, ring conformation, relative energies at the AMBER and B3LYP/6-31+G**//SM5.42/HF/6-31G* levels of theory as well as contribution to the Boltzmann distribution are also shown.

constants as the calculated values are above, below and close to the experimental values in the different cases.

III. Discussion

A. Ring Conformation. Table 5 collects the calculated, experimental, and simulated $^3J_{H,H}$ values for **1** and **2**. Observed $^3J_{H,H}$ values were measured from 1H NMR spectra of **1** and **2** dissolved in CD_3OD . At 600 MHz, there was sufficient spectral resolution of nearly all of the resonances so that coupling constants could be conveniently extracted from the one-dimensional 1H NMR spectra. The only exception was the H_2 , H_3 , and H_5 resonances of **1** that showed significant chemical shift overlap. To confirm the assigned coupling constants associated with the H_2 , H_3 , and H_5 nuclei in **1** and generally to support the assigned $^3J_{H,H}$ couplings in **1** and

2, the program NMRSim³⁷ was used to simulate the one-dimensional 1H NMR spectra. The experimental and simulated spectra were then compared by visual inspection.

The relative agreement between the experimental and simulated $^3J_{H,H}$ values provided an additional check on the accuracy of the observed coupling constants. As noted in Table 5, the errors in the measurement of the coupling constants were ± 0.19 Hz for **1** and ± 0.38 Hz for **2**. These values were the result of the digital resolution in the acquisition of the free induction decays for **1** and **2**. The average deviation of the simulated $^3J_{H,H}$ values (± 0.11 Hz for **1** and ± 0.21 Hz for **2**) is within the coupling constant error in each case. Despite this fact, for both **1** and **2**, there are examples of significant discrepancies

(37) NMRSim v4.1 as part of TOPSPIN v1.1, Brüker Biospin GmbH.

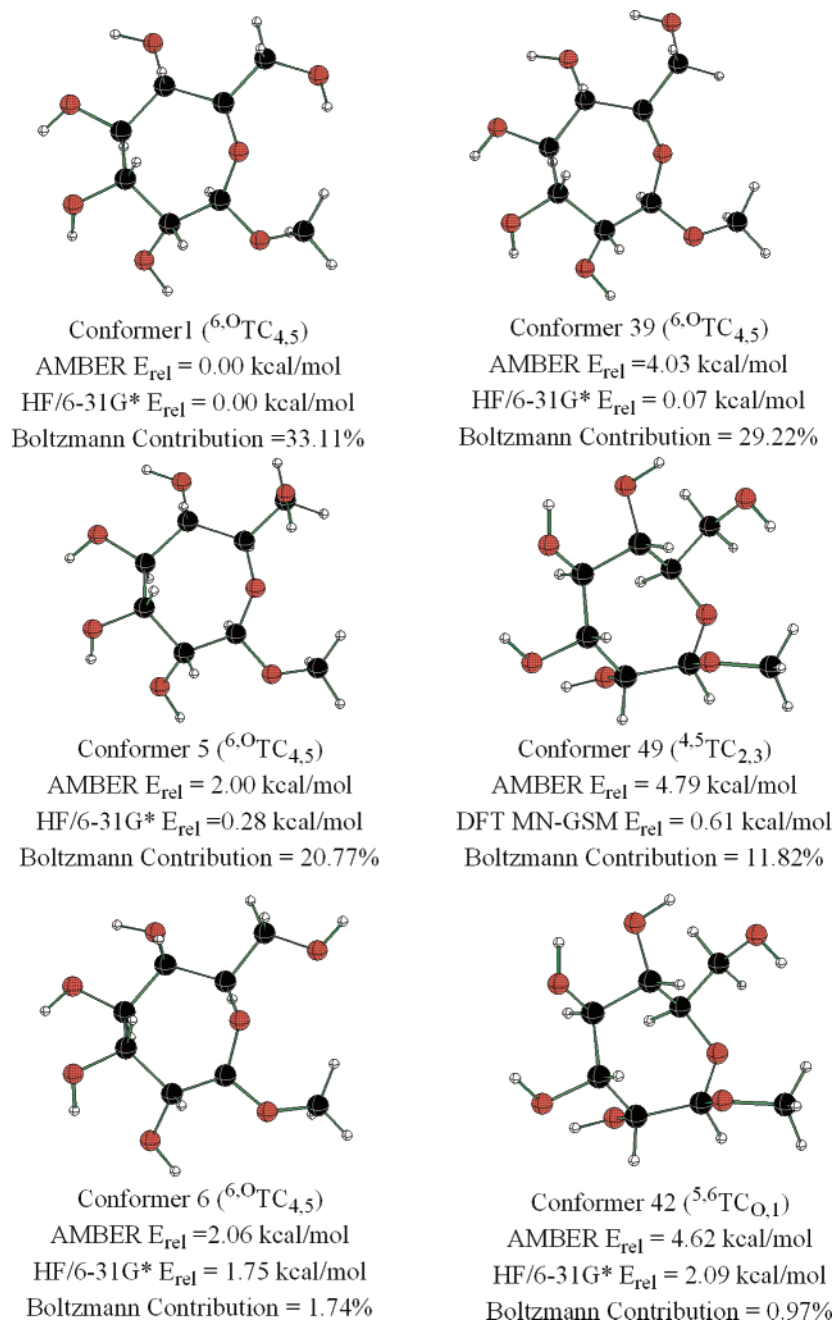


FIGURE 4. Low energy conformers of β anomer **2** in the gas phase (HF/6-31G*). The conformer number, ring conformation, relative energies at the AMBER and HF/6-31G* levels of theory as well as the contribution to the Boltzmann distribution are shown.

between the experimental and simulated values; specifically, the simulated ${}^3J_{1,2}$ was -0.25 Hz and ${}^3J_{2,3}$ was -0.22 Hz for **1** and ${}^3J_{2,3}$ was $+0.46$ Hz and ${}^3J_{5,6}$ was -0.92 Hz for **2**. Interestingly, in each of these cases, the simulated values deviated in the direction of the deMon calculated values. Overall, the consistency between the calculated deMon values and the experimental or simulated ${}^3J_{H,H}$ values supported both the stereochemical and conformational assignment of **1** and **2**.

Both **1** and **2** showed characteristic features that governed their ring conformation. For example, the ${}^3,4TC_{5,6}$ conformation adopted by **1** placed the aglycon OCH_3 group in the isoclinal position. Compound **1** is an α -septanoside with an axial aglycon group. As previously

mentioned, bulky substituents will prefer the isoclinal position due to the diminished steric interactions at that position. Additionally, the axial OCH_3 group benefits from stabilization via the anomeric affect in **1**. In the ${}^3,4TC_{5,6}$ conformer, the other ring substituents (C_2-C_6) maintain an equatorial disposition, which alleviates steric interactions and allows the possibility of intramolecular hydrogen bonding. For β -septanoside **2**, all of the substituents are able to assume a similar equatorial disposition when the ring adopts the ${}^6,0TC_{4,5}$ conformation.

B. C_6-C_7 Rotamer Populations. Rotation about the exocyclic hydroxymethyl group has been correlated with ring conformations in several furanose systems.³⁸ Our

TABLE 4. Calculated Conformational Distribution for the β Septanoside Anomer (**2**) in the Gas Phase^a

conformer	E_{rel} AMBER	E_{rel} HF/6-31G*	ring conformation	C ₆ -C ₇ rotamer	Boltzmann contribution ^b (%)
1	0.00	0.00	6,0TC _{4,5}	gt	33.11
39	4.03	0.07	6,0TC _{4,5}	tg	29.22
5	2.00	0.28	6,0TC _{4,5}	gg	20.77
49	4.79	0.61	4,5TC _{2,3}	gg	11.82
6	2.06	1.75	6,0TC _{4,5}	gt	1.74
42	4.62	2.09	5,6TC _{0,1}	tg	0.97
51	4.97	2.43	4,5TC _{2,3}	tg	0.54
2	0.60	2.52	5,6TC _{0,1}	gt	0.47
54	5.02	2.62	3,4TC _{5,6}	gt	0.39
47	4.76	2.67	6,0TC _{4,5}	tg	0.37
3	1.00	2.92	4,5TC _{2,3}	gt	0.24
40	4.14	3.20	6,0TC _{4,5}	gt	0.15
37	3.73	3.29	6,0TC _{4,5}	gg	0.13
41	4.57	3.83	5,6TC _{0,1}	gg	0.05
9	2.29	3.86	6,0TC _{4,5}	gt	0.05
13	3.11	3.92	6,0TC _{4,5}	gg	0.04
38	4.00	4.42	4,5TC _{2,3}	gt	0.02
26	3.66	5.16	4,5TC _{2,3}	gt	0.01
52	4.98	5.29	4,5TC _{2,3}	gg	0.00
14	3.59	5.38	4,5TC _{2,3}	gt	0.00
46	4.73	5.96	6,0TC _{4,5}	gt	0.00
12	3.09	6.68	5,6TC _{0,1}	gt	0.00

^a Relative energies for each conformer, at each level of theory, are in kcal/mol. ^b The Boltzmann contribution, as a percentage, is determined based on the relative energies calculated at the HF/6-31G* level of theory.

TABLE 5. Calculated and Experimental ³J_{H,H} and ¹J_{C,H} Coupling Constants (Hz) for Septanosides **1** and **2**

coupling constant	calc 1 ^a	expt 1 ^{b,d}	NMRSim 1 ^c	calc 2 ^a	expt 2 ^{b,d}	NMRSim 2 ^c
³ J _{1,2}	5.81	6.2	5.95	5.92	5.4	5.44
³ J _{2,3}	8.86	9.8	9.58	5.42	3.3	3.76
³ J _{3,4}	7.48	8.3	8.41	9.11	9.2	9.11
³ J _{4,5}	7.17	8.3	8.36	7.38	7.2	7.32
³ J _{5,6}	8.5	10.2	10.14	8.32	9.6	8.68
³ J _{6,7R}	3.08	5.2	5.26	3.68	6.7	6.7
³ J _{6,7S}	6.41	2.8	2.77	3.85	2.5	2.55
² J _{7R,7S}		11.7	11.76		11.8	11.76
¹ J _{C,H}	154.40	167.9		143.39	160.1	

^a Values calculated using deMon and using the B3LYP/6-31+G**//SM5.42/HF/6-31G* Boltzmann weightings from that conformational distribution. ^b Observed coupling constants from ¹H NMR experiments. ^c Values used for simulation using NMRSim. ^d Coupling constant error: ± 0.19 Hz for **1** and ± 0.38 Hz for **2**.

investigation of **1** and **2** was motivated in part by the presence of the exocyclic hydroxymethyl groups in their structures. Chart 3 shows the H-C-C-H dihedral angles for the tg, gt, and gg conformers. The coupling constants (³J_{H₆,H_{7R}} and ³J_{H₆,H_{7S}}) are diagnostic for the dihedral conformation and are described by eqs 1–3.³⁹

$$0.57X_{\text{tg}} + 9.70X_{\text{gt}} + 4.11X_{\text{gg}} = {}^3J_{\text{H}_6\text{-H}_{7\text{R}}} \quad (1)$$

$$9.79X_{\text{tg}} + 3.74X_{\text{gt}} + 0.71X_{\text{gg}} = {}^3J_{\text{H}_6\text{-H}_{7\text{S}}} \quad (2)$$

$$X_{\text{tg}} + X_{\text{gt}} + X_{\text{gg}} = 1 \quad (3)$$

The H_{7S} chemical shift was assumed to be downfield relative to H_{7R} based on previous pyranose and furanose examples.^{40,41} The determination of the coefficients for

TABLE 6. Comparison of C₆-C₇ Rotamer Populations in **1** and **2**

	1		2	
	calcd	obsd	calcd	obsd
X _{tg}	74	13	30	10
X _{gt}	11	28	32	60
X _{gg}	16	59	38	30

eqs 1 and 2 is described in the Experimental Section. Table 6 collects the rotamer populations of compounds **1** and **2** based on the conformer populations generated by computation (calcd) and by solving eqs 1–3 using the observed ³J values (obsd).

Coupling constants were also determined theoretically in order to identify the C₆-C₇ rotamer present in the compounds. The coupling between H₆ and H_{7R,S} is indicative of the C₆-C₇ rotamer. The coupling constants for the individual conformers, as well as the Boltzmann-weighted coupling constants, are summarized in Tables 7 and 8. Comparison with experiment reveals that the SM5.42/HF/6-31G* level of theory is rather poor at predicting the C₆-C₇ rotameric distribution. As can be seen, the C₆-C₇ rotamer population of the α anomer is particularly poorly predicted.

(38) (a) Gordon, M. T.; Lowary, T. L.; Hadad, C. M. *J. Am. Chem. Soc.*, **1999**, *121*, 9682. (b) Gordon, M. T.; Lowary, T. L.; Hadad, C. M. *J. Org. Chem.* **2000**, *65*, 4954. (c) McCarren, P. R.; Gordon, M. T.; Lowary, T. L.; Hadad, C. M. *J. Phys. Chem. A* **2001**, *105*, 5911.

(39) The method for determining the coefficients in eqs 1–3 is described in the Experimental Section.

(40) Bock, K.; Duus, J. Ø. *J. Carbohydr. Chem.* **1994**, *13*, 513.

(41) Serianni, A. S.; Barker, R. *Can. J. Chem.* **1979**, *57*, 3160.

TABLE 7. ${}^3J_{\text{H,H}}$ Coupling Constants (Hz) for Individual $\text{C}_6\text{--C}_7$ Rotamers for Septanoside 1

α conformer ^a	${}^3J_{\text{H}_6,\text{H}_7\text{R}}$	${}^3J_{\text{H}_6,\text{H}_7\text{S}}$	rotamer
36	2.56	8.05	tg
1	8.61	2.73	gt
5	8.61	1.72	gt
9*	8.33	1.64	gt
12	2.01	1.25	gg
22	2.43	1.00	gg
3	1.16	2.16	gg
52*	8.59	1.52	gt
4	8.35	1.46	gt
13	1.41	1.90	gg
30	2.7	1.04	gg
18	8.93	1.79	gt
20	8.77	2.52	gt
23	1.97	1.66	gg
37*	1.98	1.32	gg
26*	1.15	2.17	gg
17	1.14	2.15	gg
Overall Calculated	3.08	6.41	
Experiment	5.2	2.8	

^a Conformers from the second Monte Carlo search (as unique structures) are denoted with an asterisk.

TABLE 8. ${}^3J_{\text{H,H}}$ Coupling Constants (Hz) for Individual $\text{C}_6\text{--C}_7$ Rotamers for Septanoside 2

β conformer ^a	${}^3J_{\text{H}_6,\text{H}_7\text{R}}$	${}^3J_{\text{H}_6,\text{H}_7\text{S}}$	rotamer
1	8.12	2.29	gt
40*	2.27	7.83	tg
4	7.63	1.29	gt
3	1.11	2.13	gg
9	1.13	2.12	gg
26*	1.11	2.20	gg
8*	7.83	1.36	gt
2	8.53	2.74	gt
49*	1.48	1.70	gg
11	8.15	2.33	gt
6	9.00	2.44	gt
11*	8.17	2.22	gt
10*	8.18	2.32	gt
7	7.87	1.90	gt
27*	1.99	1.71	gg
37*	8.50	2.82	gt
14	1.31	2.21	gg
13	8.23	1.54	gt
17	1.17	2.09	gg
Overall Calculated	3.68	3.85	
Experiment	6.7	2.5	

^a Conformers from the second Monte Carlo search (as unique structures) are denoted with an asterisk.

The discrepancies between the calculated and observed $\text{C}_6\text{--C}_7$ rotamer populations in Tables 7 and 8 may be explained by considering the effects that govern them. Looking first at **1**, the difference in populations is most pronounced in changing from the tg rotamer (Chart 3) in the calculated structures to gg in solution. The high tg population may be attributed to an intramolecular H-bond in the calculated structures that may not persist in solution due to strong interactions with the solvent. Dynamics calculations have shown that solvation can play a significant role in governing rotamer populations.⁴² The preponderance of the gg rotamer observed for **1** may be explained by invoking hyperconjugation between the $\sigma_{\text{C}_6\text{--H}_6} \rightarrow \sigma_{\text{C}_7\text{--O}_7}$.⁴³ We anticipate that better agreement

(42) Kirschner, K., N.; Woods, R. J. *Proc. Natl. Acad. Sci. U.S.A.* **2001**, *98*, 10541.

(43) Juaristi, E.; Atúnez, S. *Tetrahedron* **1992**, *48*, 5941.

TABLE 9. ${}^1J_{\text{C,H}}$ at the $\text{C}_1\text{--H}_1$ Anomeric Position (Hz) in α Septanoside 1

α conformer ^a	calcd coupling constant (Hz)	$\text{C}_1\text{--H}_1$ bond length (Å)
36	154.53	1.082
12	154.3	1.082
1	153.9	1.082
3	154.42	1.082
22	154.77	1.083
5	154.51	1.083
9*	154.16	1.083
13	146.77	1.082
52*	138.85	1.087
4	138.74	1.087
30	154.37	1.082
23	155.01	1.083
37*	154.48	1.082
26*	153.73	1.082
20	153.13	1.082
18	139.05	1.087
17	147.27	1.085
Overall value (Hz)	154.40	
Experiment	167.9 ^b	

^a Conformers from the second Monte Carlo search (as unique structures) are denoted with an asterisk. ^b Coupling constant error of ± 1.5 Hz.

between calculated and experimental $\text{C}_6\text{--C}_7$ rotamer populations could be attained if the calculations included at least one solvent molecule to provide some representation of such intrinsic interactions between the solute and solvent.

There is closer agreement between the calculated and observed populations for **2** (Table 8). The preference for the gt rotamer here is primarily based on a gauche effect between O_6 and O_7 , and the gg conformer by hyperconjugation as was described for **1**. The preference for the gt conformer in **2** may also represent the formation of an H-bond between the C_7 hydroxyl group and the ring (O_6) oxygen.

C. Anomeric Orientation. Calculations were also used to determine the one-bond C–H coupling constants (${}^1J_{\text{C,H}}$) at the anomeric (C_1) position. This has been a very useful tool for the assignment of α and β anomers in pyranoses⁴⁴ and some furanoses.⁴⁵ We have postulated that it may be a useful diagnostic for the identification of the anomeric orientation in septanose rings. In the larger ring, the value of this coupling constant is reasonably correlated to the C–H bond length.⁴⁶ The results of the calculations, as well as the C–H bond lengths, are given in Tables 9 and 10. From these data, there is a distinct difference in the value of these coupling constants for the α anomer (**1**) as opposed to the β anomer (**2**). There are, however, some discrepancies in the data; the deviations appear to be in conformers which will not be populated (due to their high energy) and which will contribute very little to the actual Boltzmann distribution. It should be noted that these less stable species tend to have noticeably different bond lengths from the rest of the set, and this structural aspect may be the origin of this discrepancy.

(44) (a) Perlin, A. S.; Casu, B. *Tetrahedron Lett.* **1969**, 2921. (b) Bock, K.; Pedersen, C. J. *Chem. Soc., Perkin Trans. 2* **1974**, 293.

(45) Callam, C. S.; Gadikota, R. R.; Lowary, T. L. *J. Org. Chem.* **2001**, *66*, 4549.

(46) Wolfe, S.; Pinto, B. M.; Varma, V.; Leung, R. Y. N. *Can. J. Chem.* **1990**, *68*, 1051

TABLE 10. $^1J_{C,H}$ at the C_1-H_1 Anomeric Position (Hz) in β Septanoside **2**

β conformer ^a	calcd coupling constant (Hz)	C_1-H_1 bond length (Å)
40*	143.8	1.086
1	143.1	1.086
3	143.87	1.086
9	143.93	1.086
26*	143.97	1.086
4	142.74	1.086
8*	142.43	1.087
49*	144.04	1.086
2	144.18	1.088
27*	142.67	1.086
11	141.81	1.086
6	151.7	1.082
11*	142.25	1.086
14	143.83	1.086
10*	143	1.086
7	149.64	1.081
17	149.36	1.081
37*	151.01	1.087
13	143.43	1.088
Overall value (Hz)	143.39	
Experiment	160.1 ^b	

^a Conformers from the second Monte Carlo search (as unique structures) are denoted with an asterisk. ^b Coupling constant error of ± 1.5 Hz.

The experimental $^1J_{C,H}$ values for **1** and **2** (Tables 5, 9, and 10) proved to be sufficiently distinct so that they were diagnostic of the anomeric stereochemistry. The experimental data were collected by ^{13}C -coupled HMQC experiments where the peak separation for C_1 was measured to yield the $^1J_{C,H}$ coupling constant. The magnitudes of $^1J_{C,H}$ of **1** ($^1J_{C,H} = 167.9$ Hz) and **2** ($^1J_{C,H} = 160.1$ Hz) were comparable to reported pyranose and furanose values.^{44,45} The apparent sensitivity of the $^1J_{C,H}$ to the anomeric stereochemistry further suggested that one ring conformer was dominant for **1** and **2**, and did not suggest averaging due to conformational interconversion. Comparison of the measured with the calculated $^1J_{C,H}$ values in Tables 9 and 10 show a systematic underestimation in the magnitude of the one-bond coupling constants. However, both the measured and calculated $^1J_{C,H}$ value for **1** are greater than for **2**. This consistency between the relative differences in the measured and calculated values indicated that there is some general agreement between the two methods. Although preliminary, the results show that the magnitude of $^1J_{C,H}$ values could be diagnostic for the determination of septanoside anomeric stereochemistry.

IV. Conclusions

We have demonstrated the synthesis of methyl α -D-glycero-D-idoseptanoside (**1**) and methyl β -D-glycero-D-guloseptanoside (**2**). The route is highlighted by the use of carbohydrate-based oxepine **4** as a glycosyl donor. In contrast to our earlier report of the epoxidation of carbohydrate-based oxepines using DMDO,¹⁰ the epoxidation in the case of **4** was not stereoselective and gave a mixture of 1,2-anhydroseptanoses. The product methyl septanosides (**1** and **2**) are especially noteworthy due to the hydroxymethyl groups at the C_6 position of the ring. Because most previous synthetic preparations cyclized through the C_6 hydroxy group, the resulting septanosides

lack this functionality. We consider the exocyclic hydroxymethyl group to be an important factor for determining new low energy conformations, and for the potential biological activity of septanosides in general.

The conformational analysis of **1** and **2** has allowed for an assignment of their anomeric configuration and the determination of their respective low energy conformations. This approach for determination of the low-energy conformations involved a Monte Carlo search followed by minimization with the AMBER force field and subsequent geometric refinement at the SM5.42/HF/6-31G* and B3LYP/6-31+G** levels. Calculated $^3J_{H,H}$ coupling constants derived from a weighted Boltzmann population of the low energy conformations using the deMon software package provided a theoretical basis for discriminating the α and β anomers as **1** and **2**, respectively. The computational analysis indicated that only one ring conformation was accessible by **1** ($^{3,4}TC_{5,6}$) and **2** ($^{6,0}TC_{4,5}$); the main variation in the low-energy conformers was through rotation about the C_6-C_7 exocyclic bond. This finding supports previous reports that monoseptanosides may reside in one dominant, low-energy conformation. However, at this time, we are unable to provide information about the energy barrier for interconversion between the assigned low-energy conformers and their conformational variants. Overall, the results indicate that septanose carbohydrates may be less conformationally flexible than other seven-membered ring structures, and that electronic effects (anomeric, exo-anomeric, H-bonding) common to carbohydrate chemistry contribute to determining the dominant energy minima.

Gas-phase HF/6-31G* calculations predicted very little difference in the final geometries as compared to optimizations performed at the SM5.42/HF/6-31G* level of theory and provided very similar contribution to the final Boltzmann distribution. This indicates that the solvation model does not significantly affect the geometries and relative energetics of the conformers contributing to the Boltzmann distribution. In both the gas-phase and aqueous-phase calculations, intramolecular hydrogen bonding appears to be very significant in the most preferred conformations of **1** and **2**.

The computational results are supported by experimental 1H NMR spectroscopic data. The correspondence between the calculated, observed, and simulated $^3J_{H,H}$ values allowed for the assignment of the α and β anomers as **1** and **2**, respectively, and confirm the accuracy of the conformations provided by computation. Analysis of the $C_6-C_{7R,S}$ coupling constants allowed for the reassignment of the rotamer populations. The discrepancy between the calculated and experimental results for the $C_6-C_{7R,S}$ coupling constants was based on the fact that the computational treatment over-predicted the tg rotamer in both **1** and **2**; a situation in which the tg rotamer was involved in intramolecular hydrogen bonding with the C_5 hydroxyl group. On the other hand, in our NMR experiments, the methanol solvent could effectively compete as an H-bond acceptor and therefore favor alternative rotameric conformations around the C_6-C_7 bond.

We are currently exploring the synthesis of di- and oligoseptanosides using the strategies we have described here and the conformational analysis of these structures. The goal of these investigations is to utilize septanose carbohydrates as inhibitors of biologically important

carbohydrate processing enzymes and as the basis for developing new protein–carbohydrate interactions that are orthogonal to natural systems.

V. Experimental Section

1,2-Anhydro-3,4,5-tetra-*O*-benzyl- α/β -D-glycero-D-ido-guloseptanose (5). Oxepine **3** (0.029 g, 0.054 mmol) was dried via azeotropic distillation from toluene (3 \times 5 mL) under reduced pressure and dissolved in dry DCM (2 mL). The solution was cooled in an ice bath to 0 °C and a DMDO (0.310 mL, 0.35 M) solution was added dropwise. The mixture was stirred at 0 °C for 30 min and the solvent was removed under reduced pressure. NMR showed quantitative conversion: ¹H NMR (CDCl₃) δ 7.44–7.32 (m, 15H), 4.88 (d, J = 11.2 Hz, 1H), 4.85 (d, J = 13.2, 1H), 4.80 (d, J = 2.2 Hz, 1H), 4.75 (d, J = 11.5 Hz, 1H), 4.69 (d, J = 9.8 Hz, 1H), 4.60 (d, J = 11.5 Hz), 3.85 (dd, J = 13.1, 3.5 Hz, 1H), 3.77 (m, 2H), 3.67 (dd, J = 13.1, 6.6 Hz, 1H), 3.56 (m, 1H), 2.99 (s, 1H); ¹³C NMR (CDCl₃) δ 138.6, 138.1, 128.7, 128.6, 128.3, 128.1, 127.9 (2), 82.3, 80.6, 79.8, 78.3, 75.4, 73.6, 73.0, 64.1, 58.4.

Methyl 3,4,5,7-Tetra-*O*-benzyl- α -D-glycero-D-ido-septanose (6) and Methyl 3,4,5,7-Tetra-*O*-benzyl- β -D-glycero-D-guloseptanose (7). DMDO epoxidation of **3** (0.039 g, 0.09 mmol) in CH₂Cl₂ (2 mL) at 0 °C over 30 min was followed by solvent removal under reduced pressure. To the residue was added NaOCH₃ (0.006 g) in CH₃OH (3 mL), and the mixture was stirred overnight (12 h). The reaction was quenched with water (2 mL), and the solvent was removed under reduced pressure. The residue was dissolved in CH₂Cl₂ (15 mL), washed with water (2 \times 15 mL), and dried (Na₂SO₄), and the solvent was removed under reduced pressure. The residue was purified by column chromatography (3:1 hexanes/EtOAc) to give two products.

Methyl 3,4,5,7-Tetra-*O*-benzyl- α -D-glycero-D-ido-septanose (6). The first fraction gave **6** (0.0084 g, 16%) as a white solid: R_f 0.32 (3:1 hexanes/EtOAc); mp 92–94 °C; [α]_D +23.6 (c 1.43, CHCl₃); ¹H NMR 400 MHz (CDCl₃) δ 7.34–7.26 (m, 18H), 7.14–7.12 (m, 2H), 4.99 (d, J = 11.1 Hz, 2H), 4.81 (d, J = 11.1 Hz, 1H), 4.80 (d, J = 10.8 Hz, 1H), 4.67–4.55 (m, 4H), 4.51 (d, J = 6.0 Hz, 1H), 3.86–3.78 (m, 2H), 3.77 (dd, J = 10.2, 3.3 Hz, 1H) 3.66–3.60 (m, 4H), 3.46 (s, 1H), 2.99 (s, 1H); ¹³C NMR 100 MHz (CDCl₃) δ 138.8, 138.5, 138.1, 137.8, 128.9, 128.6(3), 128.3(2), 128.0, 127.9(3), 127.7, 127.6, 104.3, 88.8, 79.8(2), 76.6, 76.2, 75.3, 73.7, 72.9, 70.5, 69.7, 56.1; FAB-MS m/z (M – H)⁺ calcd 583.2696, found 583.2674.

Methyl 3,4,5,7-Tetra-*O*-benzyl- β -D-glycero-D-guloseptanose (7). The second fraction gave **7** (0.025 g, 47%) as a clear colorless oil: R_f 0.24 (3:1 hexanes/EtOAc); [α]_D +23.9 (c 0.45, CHCl₃); ¹H NMR 400 MHz (CDCl₃) δ 7.33–7.27 (m, 18H), 7.18–7.17 (m, 2H), 4.72 (d, J = 11.5 Hz, 1H), 4.60–4.54 (m, 4H), 4.51–4.46 (m, 3H), 4.31 (d, J = 11.3 Hz, 1H) 4.04–4.03 (m, 2H), 3.96–3.95 (m, 2H), 3.69 (d, J = 9.1 Hz, 1H) 3.61–3.57 (m, 2H), 3.54 (s, 3H); ¹³C NMR 100 MHz (CDCl₃) δ 138.6, 138.3, 138.1, 128.6(2), 128.5, 128.2(2), 128.1, 128.0, 127.9(2), 127.7, 106.9, 81.3, 79.2, 77.8, 77.6, 73.9, 73.5, 72.9, 72.8(2), 71.7, 56.5; FAB-MS m/z (M + H)⁺ calcd 585.2852, found 585.2883.

Methyl α -D-glycero-D-Idoseptanose (1). Pd/C (10%, 0.006 g) was added to a solution of **6** (0.021 g, 0.036 mmol) in CH₃OH (10 mL). The reaction was placed under an H₂ atmosphere via a balloon, and the mixture was stirred for 4 h at rt. The balloon was removed from the flask, and the mixture was filtered through a short pad of Celite. The Celite was washed with additional CH₃OH (4 \times 5 mL). The solvent was removed from the combined filtrates by rotary evaporation under reduced pressure to give a clear, colorless glass (0.0078 g, 95%): [α]_D +106.8 (c 0.24, CH₃OH); ¹H NMR 600 MHz (CD₃OD) δ 4.35 (d, J = 6.2 Hz, 1H), 3.79 (dd, J = 11.7, 2.8 Hz, 1H), 3.64 (dd, J = 11.7, 5.2 Hz, 1H), 3.56 (ddd, J = 10.2, 5.2, 2.8 Hz, 1H) 3.46 (s, 3H), 3.47–3.41 (m, 3H), 3.24 (dd, J = 8.3, 8.3 Hz, 1H); ¹³C NMR 100 MHz (CD₃OD) δ 106.2, 81.3, 74.7,

73.8, 72.4, 71.6, 64.1, 56.4; FAB-MS m/z (M + H)⁺ calcd 225.0974, found 225.0988.

Methyl β -D-glycero-D-Guloseptanose (2). Pd/C (10%, 0.009 g) was added to a solution of **7** (0.028 g, 0.047 mmol) in CH₃OH (10 mL). The reaction was placed under an H₂ atmosphere via a balloon, and the mixture was stirred for 4 h at rt. The balloon was removed from the flask, and the mixture was filtered through a short pad of Celite. The Celite was washed with additional CH₃OH (4 \times 5 mL). The solvent was removed from the combined filtrates by rotary evaporation under reduced pressure to give a clear, colorless oil (0.010 g, 98%): [α]_D +7.8 (c 1.01, CH₃OH); ¹H NMR 600 MHz (CD₃OD) δ 4.33 (d, J = 5.4 Hz, 1H), 3.83 (dd, J = 11.8, 2.6 Hz, 1H), 3.80 (dd, J = 5.4, 4.0 Hz, 1H) 3.70 (dd, J = 9.1, 7.3 Hz, 1H), 3.67 (dd, J = 9.1, 4.0 Hz, 1H), 3.57 (dd, J = 11.6, 6.7 Hz, 1H), 3.48 (ddd, J = 8.3, 6.7, 2.6 Hz, 1H), 3.43 (s, 3H), 3.29 (dd, J = 8.3, 7.3 Hz, 1H); ¹³C NMR 150 MHz (CD₃OD) δ 110.0 82.0, 75.7, 75.6, 73.9, 72.0, 64.5, 56.7; FAB-MS m/z (M + H)⁺ calcd 225.0974, found 225.0992.

NMR Spectroscopy for Conformational Analysis. NMR spectra used in the conformational analysis of **1** and **2** were recorded on samples at 5–10 mM concentration in 0.75 mL CD₃OD. The ³J_{H,H} values were measured from 600 MHz ¹H NMR spectra. Simulation of the ¹H NMR spectra for **1** and **2** was done using NMRsim from Bruker.³⁷ Overlays comparing the simulated to the observed spectra are provided in the Supporting Information. The ¹J_{C,H} were measured from ¹³C-coupled HMQC spectra. These HMQC spectra for **1** and **2** are also provided in the Supporting Information.

Determination of the C₆–C₇ Rotamer Populations. Equations 1–3 were used to determine the rotamer populations about the C₆–C₇ bond by analysis of the ³J_{H,H} coupling constants between H₆ and H_{7R} (³J_{H₆,H_{7R}) and H₆ and H_{7S} (³J_{H₆,H_{7S}). The coefficients for these equations were determined using eq 4.⁴⁷ Coefficients derived using other methods⁴⁸ were too large to fit the observed coupling constants and gave negative rotamer populations. Measured values of the H–C–C–H dihedral angles (ϕ) from the calculated low energy conformers of **1** and **2** were used to define the calculated ³J_{H₆,H_{7R} and ³J_{H₆,H_{7S} for the tg, gt, and gg rotamers.}}}}

$$J_{\text{calcd}} = J_0 \cos^2 \phi - 0.28 \text{ Hz}; J_0 = 9.27 \text{ for } 0^\circ = \phi = 90^\circ, \\ J_0 = 10.36 \text{ for } 90^\circ = \phi = 180^\circ \quad (4)$$

Acknowledgment. M.P.D. acknowledges partial support by a GAANN fellowship and a Procter and Gamble fellowship. C.M.H. gratefully acknowledges generous computational resources at the Ohio Supercomputer Center where all of these calculations were performed and thanks the National Science Foundation and the OSU Environmental Molecular Science Institute (CHE-0089147) for general support. M.W.P. thanks the University of Connecticut for financial support. We thank BrukerBioSpin Corp., Billerica, MA, for generously supplying NMR time and technical assistance in the collection of data on compounds **1** and **2**.

Supporting Information Available: ¹H and ¹³C NMR spectra for **1**, **2**, and **5–7**. ¹³C-Coupled HMQC and NMRsim overlays for **1** and **2**. Summary of energies, geometries, vibrational frequencies, and NMR coupling constants for each conformer. This material is available free of charge via the Internet at <http://pubs.acs.org>.

JO048932Z

(47) Blackburn, B. J.; Grey, A. A.; Smith, I. C. P.; Hruska, F. E. *Can. J. Chem.* **1970**, *48*, 2866.

(48) (a) Haasnoot, C. A. G.; de Leeuw, F. A. A. M.; de Leeuw, H. P. M.; Altona, C. *Recl. Trav. Chim. Pays-Bas* **1979**, *98*, 576. (b) Altona, C.; Sundaralingam, M. *J. Am. Chem. Soc.* **1973**, *95*, 2333.